# Identification of a Met-Binding Peptide from a Phage Display Library

Ping Zhao,[1] Tessa Grabinski,[1] Chongfeng Gao,[2] R. Scot Skinner,[5] Troy Giambernardi,[4] Yanli Su,[2] Eric Hudson,[3] James Resau,[3] Milton Gross,[5] George F. Vande Woude,[2] Rick Hay,[4] and Brian Cao[1]

**Abstract** **Purpose:** Aberrant c-Met expression has been implicated in most types of human cancer. We are developing Met-directed imaging and therapeutic agents.

**Experimental Design:** To seek peptides that bind specifically to receptor Met, the Met-expressing cell lines S114 and SK-LMS-1 were used for biopanning with a random peptide phage display library. Competition ELISA, fluorescence-activated cell sorting analysis, an internalization assay, and a cell proliferation assay were used to characterize a Met-binding peptide *in vitro*. To evaluate the utility of the peptide as a diagnostic agent *in vivo*, $^{125}$I-labeled peptide was injected i.v. into nude mice bearing s.c. xenografts of the Met-expressing and hepatocyte growth factor (HGF)/scatter factor – expressing SK-LMS-1/HGF, and total body scintigrams were obtained between 1 and 24 h postinjection.

**Results:** One Met-binding peptide (YLFSVHWPPLKA), designated Met-pep1, reacts with Met on the cell surface and competes with HGF/scatter factor binding to Met in a dose-dependent manner. Met-pep1 is internalized by Met-expressing cells after receptor binding. Met-pep1 inhibits human leiomyosarcoma SK-LMS-1 cell proliferation *in vitro*. In SK-LMS-1 mouse xenografts, tumor-associated activity was imaged as early as 1 h postinjection and remained visible in some animals as late as 24 h postinjection.

**Conclusions:** Met-pep1 specifically interacts with Met: it is internalized by Met-expressing cells and inhibits tumor cell proliferation *in vitro*; it is a potential diagnostic agent for tumor imaging.

Since the discovery of the c-*Met* proto-oncogene more than 20 years ago, c-*Met* and its gene product Met have been extensively studied in terms of their relevance to cancer biology (1, 2). Activation of Met via autocrine, paracrine, or mutational mechanisms can lead to tumorigenesis and metastasis (3 – 9). Numerous studies have linked inappropriate expression of this ligand-receptor pair to most types of human solid tumors, including those of brain (10), breast (11, 12), ovary (13), thyroid (14), pancreas (15), stomach (16), prostate (17), and nasopharyngeal carcinoma (18).

Neutralizing mouse monoclonal antibodies (mAb) (19) and human mAbs (20) against human hepatocyte growth factor (HGF)/scatter factor (SF) have been generated and have shown high affinities to HGF/SF in inhibiting HGF-mediated cell proliferation, survival, and invasion *in vitro* and tumor growth in animal models. Mouse anti-Met mAbs were developed as nuclear-imaging agents in xenograft mouse models (21, 22). Monoclonal antibodies have become the most rapidly expanding class of pharmaceuticals for treating a wide variety of human cancers, but poor tumor penetration of antibodies due to the size of molecules, as well as liver/bone marrow toxicity by nonspecific uptake of the antibodies, has limited applications (23 – 25). Over the past decade, antibody engineering has made remarkable progress for tumor diagnosis and therapy. Antibody fragments and peptidic-targeting agents have been successfully developed by using combinatorial libraries displayed on microorganisms (26 – 32). Compared with antibodies and the fragments, peptides (1-2 kDa) are considerably smaller, generally do not bind to the reticuloendothelial system, and should not elicit an immune response upon repeated administration (33, 34). Therefore, peptides are promising molecules for delivering radionuclides or therapeutic drugs into tumors.

Peptidic agonists have been selected by screening peptide libraries against purified cell surface molecules (35 – 38). However, functionally folded soluble extracellular domains of some target membrane proteins have been difficult to obtain. In addition, because cell surface proteins are frequently posttranslationally modified, peptides selected against purified recombinant protein may not be able to access their targets on living cells (39). Therefore, some specific ligands for cell surface targets have been discovered by biopanning on whole intact cells (40 – 43).

The aim of this study was to seek a Met-binding peptide that could be used as a diagnostic agent and possibly as a therapeutic carrier. A random peptide phage display library was used to identify a Met-binding peptide by a subtractive

**Authors' Affiliations:** Laboratories of [1]Antibody Technology, [2]Molecular Oncology, [3]Analytical, Cellular, and Molecular Microscopy, and [4]Noninvasive Imaging and Radiation Biology, Van Andel Research Institute, Grand Rapids, Michigan and [5]Nuclear Medicine Service, Department of Veterans Affairs Healthcare System, Ann Arbor, Michigan

Received 1/8/07; revised 7/18/07; accepted 8/9/07.

**Grant support:** Jay and Betty Van Andel Foundation of the Van Andel Research Institute and the Michigan Economic Development Corporation.

The costs of publication of this article were defrayed in part by the payment of page charges. This article must therefore be hereby marked *advertisement* in accordance with 18 U.S.C. Section 1734 solely to indicate this fact.

**Requests for reprints:** Brian Cao, Van Andel Institute, 333 Bostwick Avenue, N.E. Grand Rapids, MI 49503. Phone: 616-234-5342; Fax: 616-234-5343; E-mail: brian.cao@vai.org.



doi:10.1158/1078-0432.CCR-07-0035

panning approach on intact cells. Specificity and affinity of this peptide were examined by a number of *in vitro* assays. Nuclear imaging of the radiolabeled peptide in mouse xenograft model exhibited tumor-associated activity, recommending this peptide as a promising candidate for future clinical applications.

## Materials and Methods

***Reagents and cell lines.*** The Ph.D.-12 Phage Display Peptide Library kit was purchased from New England Biolabs. $^{125}$I was purchased as NaI [480-630 MBq (13-17 mCi)/μg iodine] from Amersham Corp.

NIH 3T3 cells, S114 cells (NIH 3T3 transfected with the human genes for HGF/SF and Met; ref. 44), SK-LMS-1 (human leiomyosarcoma cell line), SK-LMS-1/HGF cells (human leiomyosarcoma cell line autocrine for human Met and human HGF/SF; ref. 45), MKN45 (human gastric carcinoma), DU145 and PC3 (paracrine Met-expressing human prostate carcinoma) cells were cultured in DMEM supplemented with 10% fetal bovine serum.

***Selection and amplification of Met-binding phage.*** Biopanning was carried out by using a subtractive whole-cell approach. S114 and the parental NIH 3T3 cells in log-phase growth were detached with cell dissociation buffer (Invitrogen) and were blocked with blocking buffer (PBS with 1% bovine serum albumin). Ph.D.-12 random peptide–displayed phage ($1.5 \times 10^{11}$ plaque-forming unit) were incubated with $1.0 \times 10^7$ NIH 3T3 cells for 30 min at room temperature (RT). Cells were spun down, and the depleted phage supernatant was transferred to blocked S114 cells ($1.0 \times 10^7$ cells) and incubated for 1 h (30 min for the subsequent rounds) at RT with gentle agitation. The cells were spun down and washed thrice with PBS. Cell-bound phage were eluted by incubation with 0.5 mL PBS containing 0.05% trypsin and 0.53 mmol/L EDTA for 5 min at 37°C. The eluted phage were amplified and precipitated according to New England Biolabs' instruction. The second round panning was carried out with SK-LMS-1/HGF cells; the third and fourth round were carried out with S114 and SK-LMS-1/HGF cells, respectively, to ensure the specificity of selected clones.

***Phage capture ELISA and competitive ELISA.*** The specificity of individual peptide-display phage for Met binding was assessed by phage ELISA. Human Met-Fc fusion protein (R&D Systems) was coated at a final concentration of 0.4 μg/mL. Single plaques of phage were picked up randomly and amplified in 2 mL of ER2738 culture for 4.5 h. The culture supernatant was added to the coated plates and incubated at RT for 1 h, followed by horseradish peroxidase–conjugated anti-M13 IgG (Amersham), and the plates were incubated for 1 h at RT. After washing, TMB substrate (Pierce) was used according to manufacturer's instructions.

For competitive ELISA, HGF samples (25 μg/mL) mixed with or without phage clones ($2 \times 10^{11}$ plaque-forming unit per mL, $2 \times 10^{12}$ plaque-forming unit per mL), with or without Met-pep1 (10, 100, 500 μmol/L) were incubated on the Met-coated plates for 1.5 h at RT and detected by an in-house rabbit anti-HGF polyclonal antibody. Nonavid control peptide was tested at the concentration of 500 μmol/L. Alkaline phosphatase–conjugated antirabbit IgG (Sigma) were added and phosphatase substrate CP-nitrophenyl phosphate (Kirkegaard & Perry Laboratories) was added for 30 min, and absorbance was measured at 405 nm.

***DNA sequencing and peptide synthesis.*** Single-stranded phage DNA was prepared from ELISA-positive clones as described in the phage display peptide library manual. DNA sequencing was carried out in a 3700 DNA Analyzer (Applied Biosystems) following the manufacturer's instructions.

Peptides representing the sequence of positive clone 30 (YLFSVHWPPLKA) and nonavid peptide (ASYPFLVKLWHP) and their FITC and biotin conjugates were synthesized by Genemed Synthesis, Inc.

***Fluorescence-activated cell sorting analysis.*** DU145, MKN45, NIH 3T3, and PC3 cells ($1.0 \times 10^6$) were detached with TrypLE Express (Invitrogen) and were incubated with Met-pep1-FITC or FITC-labeled nonavid peptide at a final concentration of 10 μg/mL for 15 min at 4°C. The cells were then washed twice and suspended in 500 μL PBS. Flow cytometry was done with a fluorescence-activated cell sorting Calibur cytometer and the CellQuest analysis program (Becton Dickinson).

***Fluorescent images.*** Mixed MKN45 and NIH 3T3 cells were cultured in eight-chamber slides. After fixing with 10% formalin, the cells were blocked and incubated with Met-pep1-biotin or nonavid peptide-biotin (50 μg/mL) and a specific anti-Met murine monoclonal antibody, Met4 (20 μg/mL), for 1.5 h at RT. After washing, fluorescein (DTAF)-conjugated streptavidin (Jackson ImmunoResearch) and antimouse IgG-TRITC (Jackson ImmunoResearch) were added to cells and incubated for 1.5 h at RT. Nuclei were stained with 4′,6-diamidino-2-phenylindole.

***Affinity measurement.*** The binding affinity of Met-pep1 to Met was measured by KinExA 3000. Serially diluted SK-LMS-1 cells (1:4 dilutions, starting from $16 \times 10^6$ cells per mL for curve 1 and $4 \times 10^6$ cells per mL for curve 2) were incubated with constant Met-pep1-FITC at 500 nmol/L for curve 1 or 100 nmol/L for curve 2 overnight until equilibrium was reached. Cells were removed by centrifugation. Unbound Met-pep1-FITC was retrieved by passing the supernatant fractions through Met-coated beads. Multiple curve analysis was done to determine optimal values for the equilibrium dissociation constant $K_d$ by using the KinExA Pro program.

***Internalization.*** S114 and NIH 3T3 cells were plated in eight-chamber slides. Met-pep1-biotin or nonavid peptide-biotin was added to the medium to a final concentration of 25 μmol/L for 1 or 16 h. The cells were then washed and fixed with acetone/methanol (50:50) for 10 min. After blocking, the slides were incubated with Met4 at 20 μg/mL for 1.5 h at 37°C. After washing with PBS twice, the cells were incubated with a mixture of either antimouse FITC conjugate and streptavidin–rhodamine red conjugate or DTAF-streptavidin and anti-mouse-TRITC for 1.5 h at RT. 4′,6-Diamidino-2-phenylindole was used to stain nuclei. The slides were examined by confocal laser scanning microscopy.

***Cell proliferation assay.*** SK-LMS-1 cells were seeded in 96-well plates (2,000 cells per well) and incubated for 24 h. After 12 h of serum starvation, Met-pep1 or nonavid control peptide (100 μmol/L) was

**Random peptide phage library**
↓
**Pre-absorption on NIH3T3 cells**
↓
**Biopanning on S114 and SK-LMS-1 cells alternately**
↓
**Single phage clone recovery and ELISA screening**
↓
**Sequence analysis**
↓
**Peptide synthesis**
↓
**Phage and Peptide competition ELISA**
↓
**FACS analysis and fluorescence imaging**
↓
**Internalization assay**
↓
**Cell proliferation assay**
↓
**Radionuclear imaging in Xenograft mouse**

**Fig. 1.** Schematic representation of the experimental design.

**Table 1.** Summary of Met-binding clones

| Phage clone | Peptide sequence | % Competition |
|---|---|---|
| 2 | QHKTSITGHHLEP | 28.6 |
| 3 | TLPSPLALLTVH | 39.1 |
| 30 | YLFSVHWPPLKA | 59.3 |

added at different concentrations, with or without HGF/SF (100 ng/mL), and incubated for 12 h. Finally, [$^3$H]thymidine was added for 4 h (0.5 mCi per well; PerkinElmer). [$^3$H]Thymidine incorporation was measured using a scintillation counter (MicroBeta TriLux, PerkinElmer).

***Tumor xenografts and nuclear imaging with Met-pep1.*** SK-LMS-1/HGF cells were used for xenograft induction. Female athymic nude (*nu/nu*) mice at ~2 months of age received s.c. injections of the cell suspension ($5 \times 10^5$ cells) in the posterior aspect of the right thigh. Tumors developed for 3 to 4 weeks, reaching 0.5 cm or more in greatest dimension by external caliper measurement before imaging. Mice were housed in small groups and given *ad libitum* access to mouse chow and drinking water under conditions approved by the Institutional Animal Care and Use Committee. For nuclear imaging experiments, the synthetic Met-avid peptide Met-pep1 or the nonavid control peptide was dissolved in 0.25 mol/L sodium phosphate buffer (pH 7), stored frozen in small aliquots, and thawed just before labeling. Protein radioiodination was done essentially as previously described (46).

Animals were imaged, and scintigrams were analyzed by established methods (21, 46). In brief, each mouse received $^{125}$I-labeled Met-pep1 (77 μCi, ≤0.1 mL) or control nonavid peptide (124 μCi, ≤0.1 mL) i.v. by tail vein injection under light inhalation anesthesia. Just before each imaging session, each mouse was given up to 13 mg/kg xylazine and 87 mg/kg ketamine s.c. in the interscapular region. Serial posterior whole-body gamma camera images of each mouse were acquired beginning 1 h after $^{125}$I-Met-pep1 or nonavid control peptide injection and continuing until 24 h postinjection. Sedated mice were placed in groups on top of an inverted camera head with a protective layer over the collimator and taped to the layer to maintain optimum limb extension. Images of $^{125}$I activity were acquired on a remanufactured ZLC-Scintron camera (MiE America) with a low-energy, high-sensitivity collimator. Acquisitions were obtained over a period of 30 min.

Relative activity was determined by computer-assisted region-of-interest analysis for each tumor, for total body, and for appropriate background regions at each imaging time point. These data are expressed as background-corrected and decay-corrected activity ratios. Graphical and statistical analysis of the converted data used the program Excel (Microsoft).

## Results

***Identification of peptide binders against human Met using phage display.*** A schematic representation of the experimental design is shown in Fig. 1. A 12-mer random peptide phage display library was screened with Met-expressing S114 and SK-LMS-1/HGF cells alternately to seek Met-binding peptides. NIH 3T3 cells were used for negative selection to remove nonspecific binders. After four rounds of biopanning, 30 phage clones were picked randomly for screening, all of which were found reactive against Met recombinant protein. They were then tested by competitive ELISA with or without HGF for Met binding. Three clones with the ability to compete with HGF in a dose-dependent manner for Met binding were sequenced (Fig. 2A; Table 1). Clone 30 (YLFSVHWPPLKA) displayed the highest competitive ability (59.3% inhibition as summarized in Table 1). The synthetic peptide of clone 30 (designated Met-pep1) also showed the competition ability to HGF for Met-binding in a dose-dependent fashion (Fig. 2B). At the concentration of 100 and 500 μmol/L, Met-pep1 competed 30% and 50% of HGF at 25 μg/mL for Met-binding. The nonavid peptide showed no competitive effect on HGF/Met binding (Fig. 2B).

***Met-pep1 binds Met on a live or fixed cell surface.*** The specific binding activity of Met-pep1 to Met on live Met-expressing cells was determined by fluorescence-activated cell sorting analysis. FITC-conjugated Met-pep1 specifically binds Met-expressing DU145, MKN45, and PC3 cells (Fig. 3A). Very low level of binding was observed in NIH 3T3 cells. FITC-labeled nonavid peptide did not show any binding in all cells.

Since MKN45 and NIH 3T3 cells display different morphology in culture flasks, we mixed these two cell lines when plating them in eight-chamber slides. The colocalization of Met-pep1 and an anti-Met–specific monoclonal antibody Met4 in fluorescent staining indicated that Met-pep1 binds specifically to Met on formalin-fixed MKN45 cells, but not on NIH 3T3 cells (Fig. 3B).

To determine the affinity of Met-pep1, serially diluted SK-LMS-1 cells (1:4 dilution, starting from $16 \times 10^6$ cells per mL or $4 \times 10^6$ cells per mL) were incubated with constant Met-pep1-FITC (500 nmol/L, diamonds; 100 nmol/L closed circles) until equilibrium was reached (overnight; Fig. 3C). Cells were removed by centrifugation. The percentage of Met-pep1-FITC free in the supernatant was measured by passing the supernatant through Met-coated beads. Multiple curve analysis was done to determine optimal values for the equilibrium dissociation constant $K_d$, which was 64.2 nmol/L, calculated by *n*-curve analysis using the KinExA Pro program.

***Met-pep1 internalizes Met-expressing cells via receptor binding.*** We examined the internalization of Met-pep1 by S114 cells

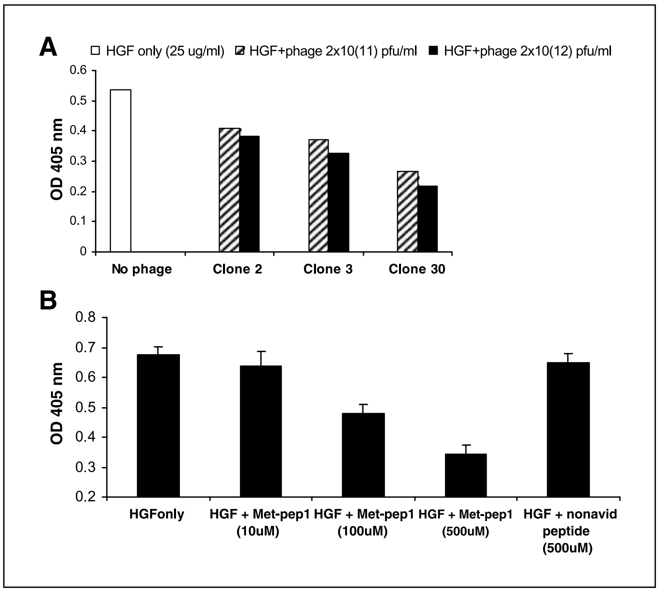


**Fig. 2.** Identification of Met-binding peptides. *A,* phage competitive ELISA. HGF samples (25 μg/mL) mixed with or without phage clones were incubated on the Met-coated plates and detected by a rabbit anti-HGF polyclonal antibody. *B,* peptide competitive ELISA. HGF samples (25 μg/mL) mixed with or without the synthetic peptide of phage clone 30 and a nonavid control peptide were incubated with Met-coated plates and detected using a rabbit anti-HGF polyclonal antibody. *Columns,* $A_{405}$ and mean of duplicate samples; *bars,* SD.

through endocytosis (Fig. 4). After incubation of S114 cells and NIH 3T3 cells with biotin-conjugated Met-pep1 for 1 and 16 h, cells were fixed and stained with fluorescein-conjugated or rhodamine red-conjugated streptavidin. Anti-Met mAb Met4 was used as a positive control for immunostaining. The green and red colors were found colocalized in S114 cells, suggesting that Met-pep1 was internalized by S114 cells via receptor binding. Internalization of Met-pep1 into S114 cells could be detected as early as 1 h, remained visible at 16 h. No internalization of Met-pep1 was found in NIH 3T3 cells. No internalization of the nonavid control peptide on both cell lines was detected (data not shown).

***Met-pep1 specifically inhibits the proliferation of human leiomyosarcoma cells.*** The exposure of Met-expressing cells to HGF/SF can elicit a variety of cellular responses including proliferation. We tested the inhibitory activity of Met-pep1 in HGF-mediated cell proliferation assay using SK-LMS cells. The cells were stimulated with HGF for 12 h before [$^3$H]thymidine was added; then [$^3$H]thymidine incorporation was measured. The results showed that 100 μmol/L of Met-pep1 clearly inhibited cell proliferation when the cells were treated with 100 ng/mL of HGF (Fig. 5). The *P* value was 0.017, calculated from Student's *t* test, indicating the differences were significant.

**In vivo *nuclear imaging with Met-pep1.*** As an additional functional test of Met-pep1 and as the first step in evaluating it as a potential *in vivo* diagnostic agent, we have conducted preliminary nuclear imaging experiments with radioiodinated Met-pep1 in nude mice bearing xenografts of the autocrine Met-HGF/SF–expressing human leiomyosarcoma cell line SK-LMS-1/HGF (Fig. 6). Five female athymic nude mice bearing s.c. xenografts of human leiomyosarcoma SK-LMS-1/HGF in the posterior aspect of the right thigh were each injected i.v. with 77 μCi $^{125}$I-Met-pep1, whereas an additional five xenograft-bearing mice were each injected i.v. with 124 μCi $^{125}$I-labeled nonavid control peptide. Sequential posterior total body nuclear images of each group of mice were obtained 1 to 24 h postinjection (Fig. 6A). Tumor-associated activity was imaged as early as 1 h after injection of $^{125}$I-Met-pep1 and remained visible in some animals as late as 24 h postinjection. Activity was highest in the gastric region (*g*) at all imaging time

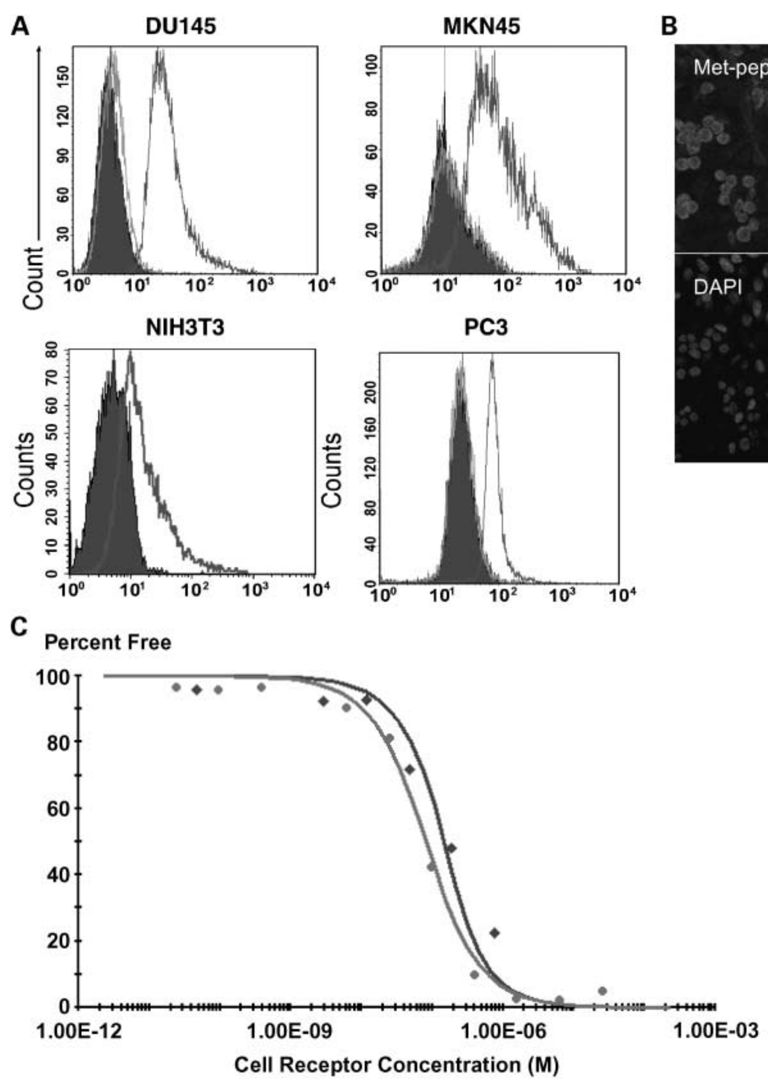


**Fig. 3.** Characterization of Met-pep1. *A,* fluorescence-activated cell sorting analysis. DU145, MKN45, NIH 3T3, and PC3 cells ($1 \times 10^6$ cells each cell line) were incubated with Met-pep1-FITC and FITC-labeled nonavid peptide (10 μg/mL) for 15 min at 4°C. *Unshaded peak,* cells incubated with Met-pep1-FITC; *grey lines,* cells incubated with FITC-labeled nonavid peptide; *shaded peaks,* unlabeled cells. *B,* fluorescent images. Mixed MKN45 and NIH 3T3 cells were cultured in eight-chamber slides. After being fixed with formalin, the cells were double-stained with Met-pep1-FITC (*green*) and a specific anti-Met monoclonal antibody Met4 (*red*). Nuclear staining with 4′,6-diamidino-2-phenylindole (*DAPI*) is also shown. *C,* affinity measurement of Met-pep1 by KinExA 3000. Serially diluted S114 cells were incubated in the presence of constant Met-pep1-FITC either at 500 nmol/L (*diamonds*) or at 100 nmol/L (*closed circles*) until equilibrium was reached. Cells were removed by centrifugation. The percentage of Met-pep1-FITC free in the supernatant was measured by passing the supernatant through Met-coated beads. Multiple curve analysis was done to determine optimal values for the equilibrium dissociation constant $K_d$.

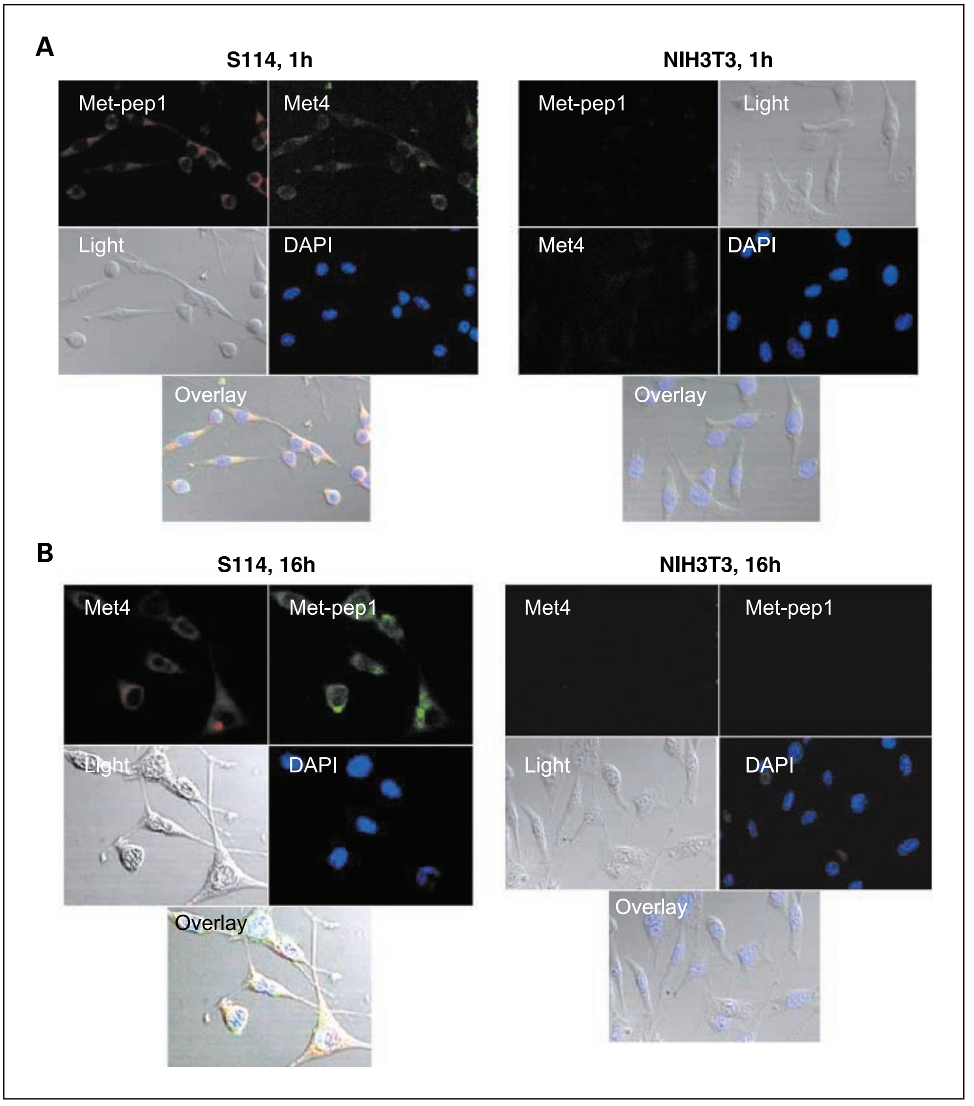


**Fig. 4.** Internalization assay. S114 and NIH 3T3 cells were plated in eight-chamber slides and cultured overnight. Met-pep1-Biotin (25 μmol/L) was added to the cells and incubated for 1 and 16 h. The cells were then washed and fixed with acetone/methanol. Met4 mAb was added to the fixed cells for positive control. Anti-mouse FITC/rhodamine and streptavidin rhodamine/FITC were used to detect Met expression.

points, whereas thyroid (*t*) activity increased over time. Activity was also evident in the nasopharyngeal (*n*) region and in the urinary bladder (*b*). The activity in the lower midline at 4 and 7 h postinjection represents the urinary bladder (*b*). By quantitative region-of-interest analysis (Fig. 6B), mean tumor-associated radioactivity accounted for 4% to 5% of the estimated injected activity of $^{125}$I-Met-pep1 at 1 and 4 h and declined to ~3% by 7 h postinjection. In contrast, mean tumor-associated radioactivity for host mice injected with $^{125}$I-labeled nonavid control peptide was only about one-third of the respective Met-pep1 values at all postinjection time points.

## Discussion

There has been an exponential growth in the development of radiolabeled peptides for diagnostic and therapeutic applications in oncology. Peptide ligands, which have the advantages of low immunogenicity, easy incorporation into certain delivery vectors, and being readily diffusible, are being pursued as targeting moieties for the selective delivery of radionuclides,

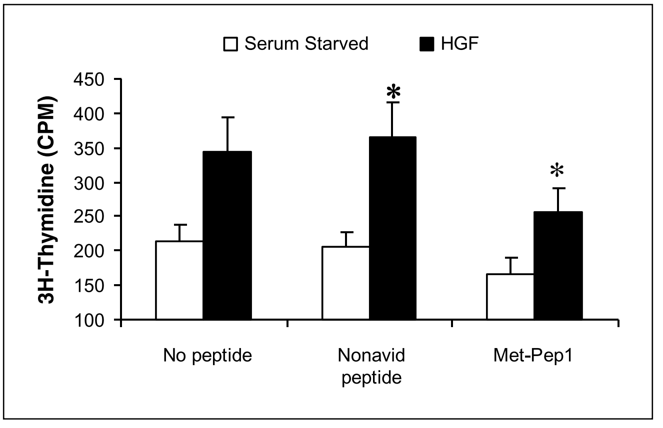


**Fig. 5.** Cell proliferation assay. SKLMS-1 cells were seeded in 96-well plates (2,000 cells per well) and cultured for 24 h. After 12 h of serum starvation, peptides were added at 100 μmol/L, with or without HGF/SF (100 ng/mL), and incubated for 12 h. Finally, [$^3$H]thymidine was added and incubated for 4 h (0.5 mCi per well). [$^3$H]Thymidine incorporation was measured by using a scintillation counter. *Columns,* cpm and means of quadruplicates; *bars,* SD. *, $P < 0.05$, compared with nonavid peptide, using Student's *t* test.

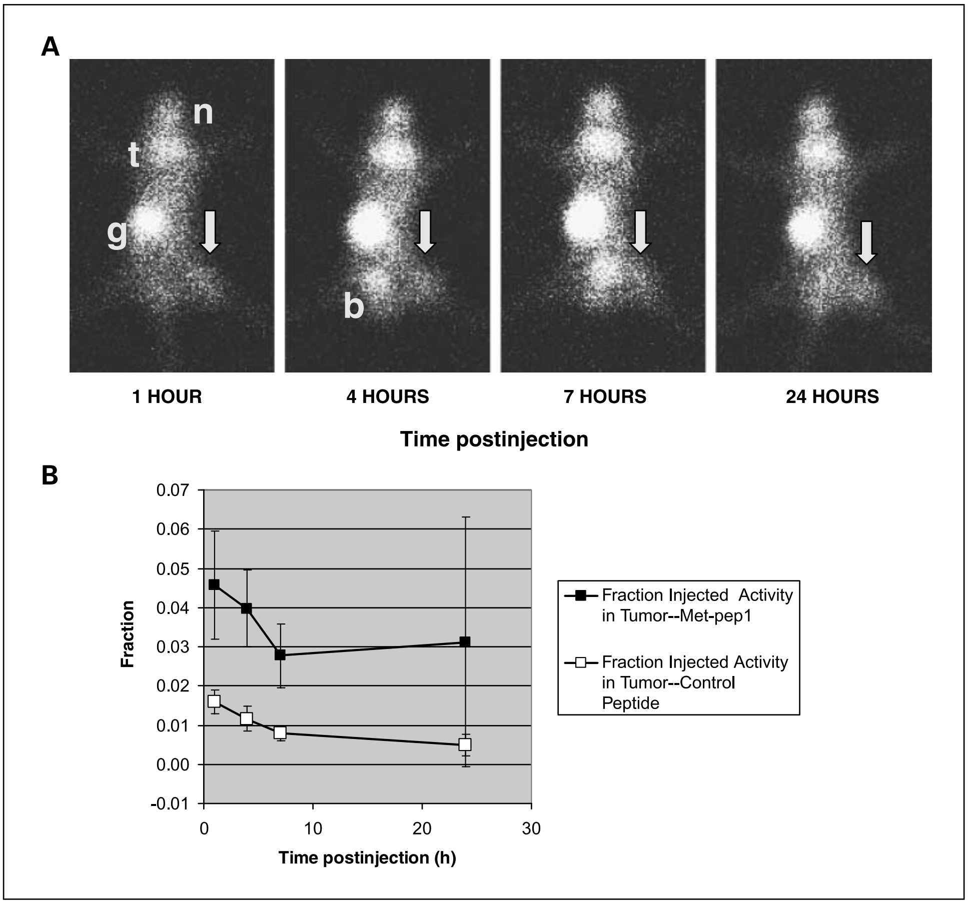


**Fig. 6.** Radionuclear imaging in Xenograft mouse. *A,* serial scintigrams of a mouse bearing human tumor xenograft autocrine for Met-HGF/SF expression. Five female athymic nude mice bearing s.c. xenografts of human leiomyosarcoma SK-LMS-1/HGF in the posterior aspect of the right thigh were injected i.v. each with 77 μCi $^{125}$I-Met-pep1. Posterior total body nuclear images were obtained 1 to 24 h postinjection. Serial images from one mouse are shown. The arrows depict the tumor xenograft location. *g,* gastric; *t,* thyroid; *n,* nasopharyngeal; *b,* urinary bladder. *B,* region-of-interest analysis. Serial scintigrams for each host animal injected with either $^{125}$I-Met-pep1 (77 μCi, *closed squares*; $n$ = 5 mice) or with $^{125}$I-labeled nonavid control peptide (124 μCi, *open squares*; $n$ = 5 mice) were evaluated by quantitative region-of-interest analysis. *Points,* mean for the fraction of injected activity postinjection found in tumors as a function of time for each group of animals; *bars,* SD.

cytokines, chemical drugs, or therapeutic genes to tumors (47). Faster blood clearance, rapid tissue penetration, and higher target-to-background ratios have been attained for peptides relative to macromolecular compounds in nuclear imaging studies. Radiolabeled receptor-binding peptides have become an accepted new class of radiopharmaceuticals (48, 49).

In this paper, we have shown through multiple approaches that Met-pep1 binds specifically to the extracellular domain of human Met, as expressed on the surface of human cancer cells *in vitro* and *in vivo*, and our data indicate that it must bind near the HGF/SF ligand binding site. Met-pep1 is internalized after its binding to Met, as evidenced both by direct imaging *in vitro* and by the liberation of free iodide *in vivo*.

To begin evaluating the diagnostic potential of Met-pep1, we conducted preliminary nuclear imaging experiments with radioiodinated Met-pep1 in nude mice bearing xenografts of the autocrine Met-HGF/SF–expressing human leiomyosarcoma cell line SK-LMS-1/HGF. We previously used this model system to evaluate full-length murine anti-Met monoclonal antibodies (Met3 and Met5) as potential radiopharmaceuticals (21, 22, 46), as well as a human Fab fragment that specifically recognizes Met (27). Consistent with the general observation that peptides display a lower affinity for a given antigen, the tumor-associated radioactivity values are lower than we reported for the radiolabeled full-length murine anti-Met mAbs and human Fab (21, 22, 27, 46), but nonetheless are higher than the levels we found for either an irrelevant full-length mAb in the same model (21) or for a nonavid control dodecameric peptide (Fig. 6B).

In conclusion, due to its specific binding to Met-expressing tumor cells *in vitro* and *in vivo* together with internalization, Met-pep1 represents a promising candidate useful for clinical Met-directed diagnostic and therapeutic applications. Coupling cytotoxic drugs to macromolecular carriers has been shown to be a promising approach for efficient drug targeting. To further develop the use of this peptide in drug delivery, conjugation of toxins to Met-pep1 and their activities in *in vitro* assays are now under way in our laboratory.

## Acknowledgments

We thank Dr. David Petillo for DNA sequencing, Rich West for running the fluorescence-activated cell sorting Calibur cytometer, and David Nadziejka for editorial reading of the manuscript.

## References

**1.** Cooper CS, Park M, Blair D, et al. Molecular cloning of a new transforming gene from a chemically transformed human cell line. Nature 1984;311:29–33.

**2.** Bottaro DP, Rubin JS, Faletto DL, et al. Identification of the hepatocyte growth factor receptor as the c-met proto-oncogene product. Science 1991;251:802–4.

**3.** Rong S, Jeffers M, Resau JH, et al. Met expression and sarcoma tumorigenicity. Cancer Res 1993;53:5355–60.

**4.** Rong S, Segal S, Anver M, et al. Invasiveness and metastasis of NIH 3T3 cells induced by Met-hepatocyte growth factor/scatter factor autocrine stimulation. Proc Natl Acad Sci U S A 1994;91:4731–5.

**5.** Takayama H, LaRochelle W, Sharp R, et al. Diverse tumorigenesis associated with aberrant development in mice overexpressing hepatocyte growth factor/scatter factor. Proc Natl Acad Sci U S A 1997;94:701–6.

**6.** Ferracini R, Olivero M, Di Renzo MF, et al. Retrogenic expression of the MET proto-oncogene correlates with the invasive phenotype of human rhabdomyosarcomas. Oncogene 1996;12:1697–705.

**7.** Wang R, Ferrell LD, Faouzi S, et al. Activation of the Met receptor by cell attachment induces and sustains hepatocellular carcinomas in transgenic mice. J Cell Biol 2001;153:1023–34.

**8.** Danilkovitch-Miagkova A, Zbar B. Dysregulation of Met receptor tyrosine kinase activity in invasive tumors. J Clin Invest 2002;109:863–7.

**9.** Birchmeier C, Birthmeier W, Gherardi E, Vande Woude GF. MET, metastasis, motility and more. Nat Rev Mol Cell Biol 2003;4:915–25.

**10.** Jung W, Castren E, Odenthal M, et al. Expression and functional interaction of hepatocyte growth factor-scatter factor and its receptor c-met in mammalian brain. J Cell Biol 1994;126:485–94.

**11.** Altstock RT, Stein GY, Resau JH, et al. Algorithms for quantitation of protein expression variation in normal versus tumor tissue as a prognostic factor in cancer: Met oncogene expression and breast cancer as a model. Cytometry 2000;41:155–65.

**12.** Tsarfaty I, Alvord WG, Resau JH, et al. Alteration of met protooncogene product expression and prognosis in breast carcinomas. Anal Quant Cytol Histol 1999;21:397–408.

**13.** Huntsman D, Resau JH, Klineberg E, et al. Comparison of c-met expression in ovarian epithelial tumors and normal epithelia of the female reproductive tract by quantitative laser scan microscopy. Am J Pathol 1999;155:343–48.

**14.** Di Renzo MF, Olivero M, Ferro S, et al. Overexpression of the c-MET/HGF receptor gene in human thyroid carcinomas. Oncogene 1992;7:2549–53.

**15.** Ebert M, Yokoyama M, Friess H, et al. Coexpression of the c-met proto-oncogene and hepatocyte growth factor in human pancreatic cancer. Cancer Res 1994;54:5775–8.

**16.** Di Renzo MF, Narsimhan RP, Olivero M, et al. Expression of the MET/HGF receptor in normal and neoplastic human tissues. Oncogene 1991;6:1997–2003.

**17.** Humphrey PA, Zhu X, Zarnegar R, et al. Hepatocyte growth factor and its receptor (c-met) in prostatic carcinoma. Am J Pathol 1995;147:386–96.

**18.** Qian CN, Guo X, Cao B, et al. Met protein expression level correlates with survival in patients with late-stage nasopharyngeal carcinoma. Cancer Res 2002;62:589–96.

**19.** Cao B, Su YL, Oskarsson M, et al. Neutralizing monoclonal antibodies to hepatocyte growth factor/scatter factor (HGF/SF) display antitumor activity in animal models. Proc Natl Acad Sci USA 2001;98:7443–8.

**20.** Burgess T, Coxon A, Meyer S, et al. Fully human monoclonal antibodies to hepatocyte growth factor with therapeutic potential against hepatocyte growth factor/c-Met-dependent human tumors. Cancer Res 2006;66:1721–9.

**21.** Hay RV, Cao B, Skinner RS, et al. Radioimmunoscintigraphy of human met-expressing tumor xenografts using Met3, a new monoclonal antibody. Clin Cancer Res 2003;9:3839–44s.

**22.** Hay RV, Cao B, Skinner RS, et al. Met5, a new monoclonal antibody for radioimmunoscintigraphy of met-expressing tumors. J Nucl Med 2003;44:178P.

**23.** Goldenberg, DM. Advancing role of radiolabeled antibodies in the therapy of cancer. Cancer Immunol Immunother 2003;52:281–96.

**24.** Trail PA, King HD, Dubowchik GM. Monoclonal antibody drug immunoconjugates for targeted treatment of cancer. Cancer Immunol Immunother 2003;52:328–37.

**25.** Reilly RM, Sandhu J, Alvarez-Diez TM, et al. Problems of delivery of monoclonal antibodies. Pharmaceutical and pharmacokinetic solutions. Clin Pharmacokinet 1995;28:126–42.

**26.** Griffiths AD, Williams SC, Hartley O, et al. Isolation of high affinity human antibodies directly from large synthetic repertoires. EMBO J 1994;13:3245–60.

**27.** Jiao Y, Zhao P, Zhu J, et al. Construction of human naïve Fab library and characterization of anti-Met Fab fragment generated from the library. Mol Biotechnol 2005;31:41–54.

**28.** Yanofsky SD, Baldwin DF, Butler JH, et al. High affinity type I interleukin 1 receptor antagonists discovered by screening recombinant peptide libraries. Proc Natl Acad Sci U S A 1996;93:7381–6.

**29.** Binetruy-Tournaire R, Demangel C, Malavaud B, et al. Identification of a peptide blocking vascular endothelial growth factor (VEGF)-mediated angiogenesis. EMBO J 2000;19:1525–33.

**30.** Brissette R, Prendergast JK, Goldstein N. Identification of cancer targets and therapeutics using phage display. Curr Opin Drug Discov Devel 2006;9:363–9.

**31.** O'Toole JM, Rabenau KE, Burns K, et al. Therapeutic implications of a human neutralizing antibody to the macrophage-stimulating protein receptor tyrosine kinase (RON), a c-MET family member. Cancer Res 2006;66:9162–70.

**32.** Shin-Young Im, Ki Su Kim, Chae-Ok Yun, et al. Generation of a rabbit V(H) domain antibody polyspecific to c-Met and adenoviral knob protein. Biochem Biophys Res Commun 2006;339:305–12.

**33.** Ania OH, Sroka TC, Chen ML, et al. Therapeutic cancer targeting peptides. Biopolymers 2002;66:184–99.

**34.** Nilsson F, Tarli L, Viti F, et al. The use of phage display for the development of tumour targeting agents. Adv Drug Deliv Rev 2000;43:165–96.

**35.** Wrighton NC, Farrell FX, Chang R, et al. Small peptides as potent mimetics of the protein hormone erythropoietin. Science 1996;273:458–64.

**36.** Cwirla SE, Balasubramanian P, Duffin DJ, et al. Peptide agonist of the thrombopoietin receptor as potent as the natural cytokine. Science 1997;276:1696–9.

**37.** Ballinger MD, Shyamala V, Forrest LD, et al. Semirational design of a potent, artificial agonist of fibroblast growth factor receptors. Nat Biotechnol 1999;17:1199–204.

**38.** Shrivastava A, von Wronski MA, Sato AK, et al. A distinct strategy to generate high-affinity peptide binders to receptor tyrosine kinases. Protein Eng Des Sel 2005;18:417–24.

**39.** Mori T. Cancer-specific ligands identified from screening of peptide-display libraries. Curr Pharm Des 2004;10:2335–43.

**40.** Barry MA, Dower WJ, Johnston SA, et al. Toward cell-targeting gene therapy vectors: selection of cell-binding peptides from random peptide-presenting phage libraries. Nat Med 1996;2:299–305.

**41.** Hart SL, Knight AM, Harbottle RP, et al. Cell binding and internalization by filamentous phage displaying a cyclic Arg-Gly-Asp-containing peptide. J Biol Chem 1994;269:12468–74.

**42.** Giordano RJ, Cardo-Vila M, Lahdenranta J, et al. Biopanning and rapid analysis of selective interactive ligands. Nat Med 2001;7:1249–53.

**43.** Zitzmann S, Mier W, Schad A, et al. A new prostate carcinoma binding peptide (DUP-1) for tumor imaging and therapy. Clin Cancer Res 2005;11:139–46.

**44.** Rong S, Oskarsson M, Faletto D, et al. Tumorigenesis induced by coexpression of human hepatocyte growth factor and the human *Met* protooncogene leads to high levels of expression of the ligand and receptor. Cell Growth Differ 1993;4:563–9.

**45.** Jeffers M, Rong S, Vande Woude GF. Enhanced tumorigenicity and invasion-metastasis by hepatocyte growth factor/scatter factor-met signaling in human cells concomitant with induction of the urokinase proteolysis network. Mol Cell Biol 1996;16:1115–25.

**46.** Hay RV, Cao, B, Skinner RS, et al. Radioimmunoscintigraphy of tumors autocrine for human Met and hepatocyte growth factor/scatter factor. Molec Imaging 2002;1:56–62.

**47.** Langer M, Beck-Sickinger AG. Peptides as carrier for tumor diagnosis and treatment. Curr Med Chem Anticancer Agents 2001;1:71–93.

**48.** de Jong M, Kwekkeboom D, Valkema R, Krenning E. Radiolabelled peptides for tumour therapy: current status and future directions. Eur J Nucl Med Mol Imaging 2003;30:463–9.

**49.** Lambert B, Cybulla M, Weiner SM, et al. Renal toxicity after radionuclide therapy. Radiat Res 2004;161:607–11.